Chapter 23

Catching the Conformational Wave: Measuring the Working Strokes of Protofilaments as They Curl Outward from Disassembling Microtubule Tips

Lucas E. Murray, Haein Kim, Luke M. Rice, and Charles L. Asbury

Abstract

Optical traps have enabled foundational studies of how mechanoenzymes such as kinesins and dynein motors walk along microtubules, how myosins move along F-actin, and how nucleic acid enzymes move along DNA or RNA. Often the filamentous substrates serve merely as passive tracks for mechanoenzymes but microtubules and F-actin are themselves dynamic protein polymers, capable of generating movement and force independently of conventional motors. Microtubule-driven forces are particularly important during mitosis, when they align duplicated chromosomes at the metaphase plate and then pull them apart during anaphase. These vital movements depend on specialized protein assemblies called kinetochores that couple the chromosomes to the tips of dynamic microtubule filaments, thereby allowing filament shortening to produce pulling forces. Although great strides have been made toward understanding the structures and functions of many kinetochore subcomplexes, the biophysical basis for their coupling to microtubule tips remains unclear. During tip disassembly, strain energy is released when straight protofilaments in the microtubule lattice curl outward, creating a conformational wave that propagates down the microtubule. A popular viewpoint is that the protofilaments as they curl outward hook elements of the kinetochore and tug on them, transferring some of their curvature strain energy to the kinetochore. As a first step toward testing this idea, we recently developed a laser trap assay to directly measure the working strokes generated by curling protofilaments. Our "wave" assay is based on an earlier pioneering study, with improvements that allow measurement of curl-driven movements as functions of force and quantification of their conformational strain energy. In this chapter, we provide a detailed protocol for our assay and describe briefly our instrument setup and data analysis methods.

Key words Kinetochore, Mitotic spindle, Anaphase, Ram's horns

1 Introduction

Optical traps have proven to be ideal tools for studying the mechanochemistry of a wide variety of biological molecules and processes. Since Arthur Ashkin's seminal work introducing the optical trap to the world [1], the technique has been used extensively to study the motions and forces produced by single kinesins and dynein on

Arne Gennerich (ed.), *Optical Tweezers: Methods and Protocols*, Methods in Molecular Biology, vol. 2478,
https://doi.org/10.1007/978-1-0716-2229-2_23,

microtubules [2–4], by myosins on F-actin fibers [5–7], by polymerases along DNA and RNA [8, 9], and many other mechanoenzymes [10–12]. Often the filamentous substrates (microtubules, F-actin, or DNA) can be considered passive tracks along which the motor enzymes move. However, in some important instances microtubules [13–17] and F-actin [18–20] can themselves produce movement and force independently of conventional motor enzymes. Here, we describe an optical trapping-based assay to measure the mechanical work output generated by individual disassembling microtubule tips (Fig. 1).

Microtubules are hollow, filamentous protein polymers that grow and shorten by addition and loss of αβ-tubulin heterodimers from their tips. Their αβ-tubulin subunits are GTP-hydrolyzing (GTPase) enzymes that associate together in two fundamental ways to form a microtubule: Longitudinal (head-to-tail) associations form protofilaments, while lateral (side-to-side) associations bridge these protofilaments, usually in groups of 13, to form the hollow microtubule body. Because free αβ-tubulin subunits adopt a curved conformation that must straighten to accommodate formation of lateral interactions with neighboring subunits in the lattice, the lattice holds strain energy [21, 22]. After GTP-tubulin heterodimers are embedded in the microtubule lattice, their GTPase activity is stimulated and the lattice is destabilized. Strained α-β-tubulin subunits trapped in the lattice can only release their stored energy during tip disassembly, when protofilaments curl outwards from the tip and splay apart. These curling protofilaments form a conformational wave that propagates down the microtubule. Lattice strain energy is fundamentally important for all current models of microtubule dynamic instability but, until recently, its magnitude could only be estimated indirectly, using thermodynamic approaches or analyses based on the bending rigidity of intact microtubules [23–25]. The assay described here provides a more direct approach.

Dynamic microtubules are also the basis of the mitotic spindle that aligns and segregates duplicated chromosomes during eukaryotic cell division [26]. The vital chromosome movements of mitosis are generated when spindle microtubules shorten, thereby pulling against specialized protein structures on each chromosome called kinetochores. The kinetochores harness energy released from disassembling microtubules by maintaining persistent, load-bearing attachments to the filament tips, even as the tips crumble beneath them [13–15]. Despite great progress in understanding the molecular structures of both kinetochore subcomplexes and microtubules, it remains unclear how kinetochores remain coupled to dynamic microtubule tips and how they harness the energy released during tip disassembly [27]. According to one of the leading models—the conformational wave model—curling protofilaments at disassembling microtubule tips physically capture and pull on

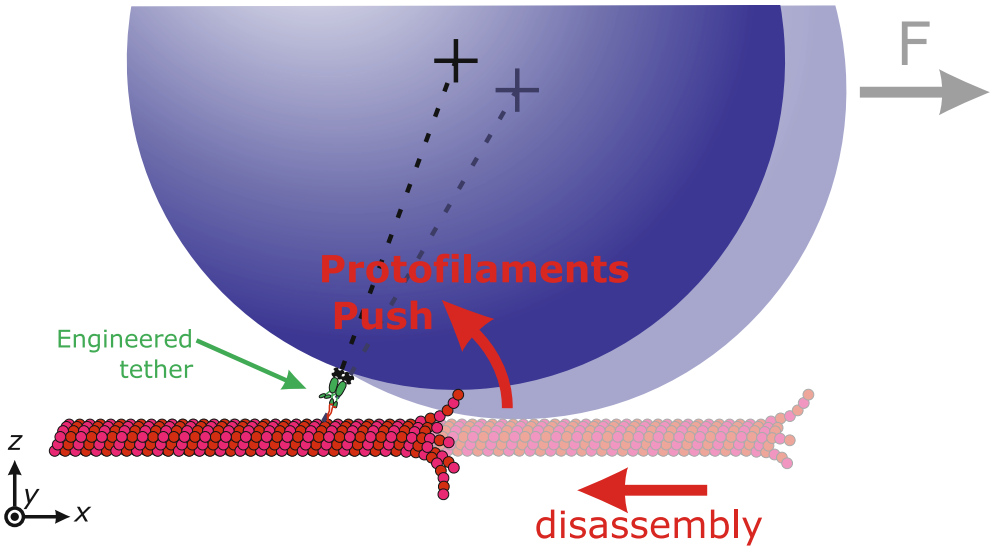

Fig. 1 Curling protofilaments at a disassembling microtubule tip cause a pulse in bead motion. A streptavidin-coated microsphere (blue with center marked by black cross) is attached to a microtubule composed of recombinant 6 × His-tagged yeast tubulin (pink and red) by an anti-penta-His antibody (green). The bead is pulled rightward with a feedback-controlled optical trap such that it rests against the side of the microtubule at a secondary contact point. When the disassembling tip reaches this secondary contact point, curling protofilaments push laterally against the bead, causing it to rotate about the tether. The bead moves initially against the force of the optical trap (i.e., leftward) before the microtubule disassembles past the tether and releases the bead. The component of motion parallel to the long axis of the microtubule (i.e., along the *x*-axis) is measured. The transverse component of motion (i.e., along the *y*- or *z*-axes) cannot be measured because the microtubule tip, which is unsupported, is not stiff enough to push the bead laterally against the transverse trapping forces

elements of the kinetochore to drive motility [13]. Alternatively, coupling could be maintained by biased diffusion, which can operate independently of any spring-like curling action of the protofilaments [28].

Using the optical trapping assay described here, we recently showed that protofilaments indeed release substantial mechanical energy as they curl outward from disassembling microtubule tips, and this energy (when extrapolated) is more than sufficient to account for kinetochore movement in vitro [29]. To measure the energy carried by the conformational wave, we modified an assay pioneered in an earlier study [30], adding a feedback-controlled laser trap and other improvements to prevent the microbeads used in the assay from restricting the curling of the protofilaments. We describe our protocol in detail here, including how to prepare a disposable channel slide sparsely decorated with coverslip-anchored microtubules, some of which have microbeads tethered to their sides. The microbeads become tethered by virtue of being sparsely decorated with recombinant tubulin, which incorporates into growing microtubule tips. This tethered bead arrangement forms a mechanical lever that amplifies the molecular-scale motions

generated by the curling protofilaments and enables their measurement in an optical trap. In addition to slide preparation and trapping procedures, we also describe data interpretation and analysis.

Because this "wave assay" provides a direct way to measure protofilament strain energy, it will be essential for testing rigorously whether curling protofilaments contribute to kinetochore-microtubule coupling. Already the assay has demonstrated the spring-like elasticity of protofilament curls, and established that they carry sufficient energy to explain microtubule-driven kinetochore motility. But rigorously testing their importance for kinetochore motility will also require modifying their energy and measuring how such modifications affect kinetochore-microtubule coupling. We envision that the wave assay will be useful for identifying assay conditions or tubulin mutants that alter wave energy and, more generally, for examining the mechanochemistry of tubulins from different organisms and/or with various posttranslational modifications.

2 Materials

2.1 Instrument Design and Optical Layout

Our instruments feature a simple fixed laser trap, with feedback control implemented via movement of a computer-controlled piezo specimen stage (Fig. 2). Video-enhanced differential interference contrast (ve-DIC) optics are included for visualization of microtubules and beads, and an additional 473-nm laser is included for optical severing of microtubules (i.e., laser "scissors"). The instruments are constructed on standard inverted research microscopes and include some custom mounting hardware. Their construction and optical layout is detailed in a prior publication [31]. This assay should be able to be performed on any microscope equipped with a feedback-controlled optical trap, cutting laser, and DIC optics for viewing individual, unlabeled microtubules.

2.2 Tubulin Purification

The wave assay as described here relies on purified, tagged recombinant yeast tubulin. A 6 × His-tag on the C-terminal tail of the β-subunit of this recombinant tubulin allows the αβ-tubulin heterodimers to be strongly tethered to streptavidin-coated microbeads functionalized with biotinylated anti-penta-His antibody. The recombinant yeast tubulin has been purified from an *S. cerevisiae* strain with an inducible overexpression system, aliquoted and snap-frozen, shipped on dry ice (from UT Southwestern to the University of Washington), and stored at −80 °C. The method for tubulin preparation is detailed in prior publications [32, 33]. Though the protocol we present relies on this recombinant yeast tubulin, any similarly tagged tubulin should work for the purposes of this assay. Our past work suggests that whatever method is used to tether

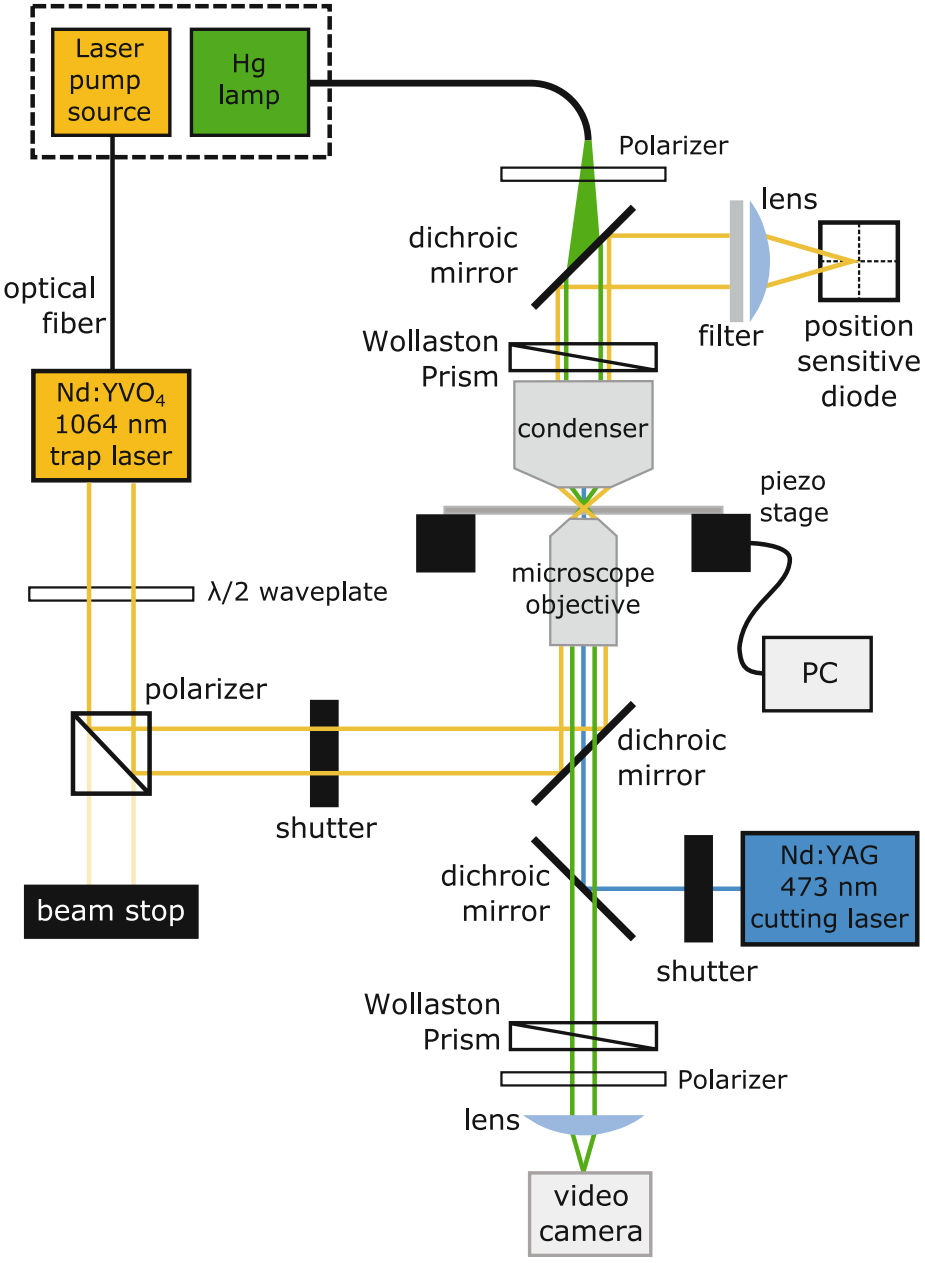

Fig. 2 Overall optical layout. The laser pump source for the 1064-nm laser and the mercury-arc lamp are located outside the microscope room (dashed box) to minimize heat and noise. The arc-lamp and laser pump beams are coupled to the instrument via optical fibers. The $\lambda/2$ waveplate and polarizer allow a fraction of the 1064-nm laser power to be selected for trapping. The trap laser enters and exits the microscope via dichroic mirrors that pass visible light. A lens projects the trapping beam through a neutral density filter onto a position sensitive diode. Trapping-beam position data is used to implement feedback by controlling the motion of the piezo specimen stage. A long-pass dichroic mirror introduces the 473-nm cutting laser into the instrument. Two Wollaston prisms and two polarizers form the DIC system. A video camera is used for contrast-enhanced DIC imaging of microtubules. Both the trapping and cutting lasers are actuated independently by operator-controlled shutters during experiments

tubulin to a microbead, a tether of sufficient length between the bead and the tubulin is required. We estimate that our tether length is approximately 36 nm when the streptavidin, antibody, and C-terminal tail of tubulin are considered. Without a source for recombinant tubulin, a tether of sufficient length could be recapitulated by linking anti-digoxygenin-coated beads to biotinylated tubulin via a bifunctional DNA molecule.

Regardless of the tethering method, waves generated by untagged tubulin (e.g., native tubulin purified from bovine brain) can be measured in the assay. The methods by which we incorporate untagged tubulin into the wave assay are described below. Purification of tubulin from bovine brain is detailed in a prior publication [34]. Alternatively, porcine brain tubulin can be purified, or tubulin can be purchased from either Cytoskeleton Inc. (Denver, CO) or PurSolutions (Nashville, TN).

2.3 Biotin-Tubulin Microtubule Seed Preparation

1. 5× BRB80 buffer: 400 mM PIPES pH 6.8, 5 mM $MgCl_2$, 2.5 mM EGTA (doi: https://doi.org/10.1101/pdb.rec086694).
2. Biotinylated porcine tubulin (Cytoskeleton Cat #T333).
3. Bovine or porcine brain tubulin (purified as in [34] or purchased from Cytoskeleton Inc., e.g., Cat. #HTS03, or from PurSolutions).
4. 10 mM GMPCPP (Jena Bioscience Cat #NU-405S).
5. Purified water (Milli-Q water, "MQ-H_2O," is used here, but double-distilled will likely suffice).
6. 40 mM 1,4-dithiothreitol (DTT) in MQ-H_2O.
7. 80% glycerol (20% in MQ-H_2O).
8. Bucket of ice.
9. Heat block equilibrated to ~30 °C.

2.4 Anti-His Bead Preparation

1. MQ-H_2O.
2. 5× BRB80 buffer: 400 mM PIPES pH 6.8, 5 mM $MgCl_2$, 2.5 mM EGTA (doi: https://doi.org/10.1101/pdb.rec086694).
3. Streptavidin-coated polystyrene beads, 440 nm in diameter, 1% weight/volume (Spherotech Cat #SVP-05-10).
4. Penta-His biotin conjugate (Qiagen Cat #34440), a mouse monoclonal IgG1 antibody that binds tightly and specifically to five (or more) consecutive Histidine residues and is conjugated to biotin.
5. 40 mg/mL Bovine serum albumin (BSA) in 1× BRB80.
6. 1 M DTT in MQ-H_2O.
7. Tip sonicator (Branson Ultrasonics Sonifier S-250A) with ½-in. diameter tip.

8. Tube rotator, placed in a cold room or refrigerated cabinet at 4 °C.
9. Benchtop centrifuge, placed in a cold room or refrigerated cabinet.

2.5 Disposable Channel Slides

1. KOH-cleaned coverslips, protocol described in prior work [31].
2. Microscope slides (Gold Seal #3011).
3. Double-stick office tape.
4. Oven (ThermoFisher PR305225G), equilibrated to 55 °C.
5. Slide humidity chamber: Briefly, a 200 μL pipette tip box is adapted to hold a disposable channel slide. Two razor blades are taped down to the tip tray to act as standoffs to support the slide. A damp paper towel is placed under the tip tray to keep enough humidity in the box to prevent rapid drying of the slide during the incubation steps described below in Subheading 3.5.

2.6 Preparing Coverslip-Anchored Microtubules with Side-Bound Microbeads

1. 5× BRB80 buffer: 400 mM PIPES pH 6.8, 5 mM $MgCl_2$, 2.5 mM EGTA (doi: https://doi.org/10.1101/pdb.rec086694).
2. Anti-His beads (prepared as described below in Subheading 3.3 using materials from Subheading 2.4 above).
3. >150 mg/mL BSA in 1× BRB80, filtered at 0.1 μm.
4. 100 mM GTP in MQ-H_2O, buffered to pH 7.
5. 5 mg/mL Biotinylated BSA (Vector Laboratories B-2007-10).
6. 1 mg/mL Avidin DN (Vector Laboratories A-3100-1).
7. Biotin-tubulin microtubule seeds (prepared as described below in Subheading 3.2, using materials describe in Subheading 2.3).
8. MQ-H_2O, filtered at 0.1 μm.
9. 40 mM DTT in MQ-H_2O.
10. 2.4 M glucose in MQ-H_2O.
11. Recombinant yeast tubulin (2–5 μM).
12. Bovine brain tubulin (assumes 190 μM) (optional, *see* Subheading 3).
13. Oxygen scavenger 100× (glucose oxidase + catalase) (Sigma Cat. #G2133, Sigma Cat #C3515): Mix to 10,000 units/mL glucose oxidase (~25 mg/mL), 100,000 units/mL catalase (~3 mg/mL), in 1× BRB80. Filter at 0.1 μm, aliquot into 5 μL volumes and freeze in liquid N_2.

14. Clear nail polish.
15. Ultracentrifuge capable of reaching 90,000 RPM at 4 °C and TLA-100 rotor (e.g., Beckman-Coulter Optima MAX-XP Ultracentrifuge and TLA-100 fixed-angle rotor) (*see* **Note 1**).

2.7 Measuring Pulses of Motion Generated by Curling Protofilaments

1. Suitable optical trap, e.g., constructed as in ref. 31. The trap should be operable in "force clamp" mode, with the force kept constant under feedback control.
2. The LabView code that we use to implement feedback can be freely downloaded from a prior publication [29], and we are happy to offer assistance or advice on its use.

3 Methods

3.1 Tubulin Purification

1. Purification of recombinant tubulin from yeast is detailed in prior publications [32, 33].
2. Purification of tubulin from bovine brain is detailed in a prior publication [34].

3.2 Biotin-Tubulin Microtubule Seed Preparation

1. Make 2× Nucleation Buffer (2× NB) (65 μL 80% glycerol, 100 μL 5× BRB80, 50 μL 10 mM GMPCPP, 10 μL 40 mM DTT, 25 μL MQ-H_2O), place on ice.
2. Reconstitute 20 μg of biotin tubulin (Cytoskeleton, Cat #T333) in 10 μL of ice-cold 1× BRB80.
3. Add 240 μg of bovine brain tubulin (12.6 μL of 190 μM bovine tubulin) to the reconstituted biotin tubulin from **step 2** (target ratio is 7–8.5% biotinylated tubulin). Add enough 1× BRB80 to make the final volume 50 μL, yielding a concentration of 4–5 μM tubulin.
4. Mix 40 μL of the tubulin mix from **step 3** with 250 μL 2× NB and 210 μL of MQ-H_2O. Final concentrations in the seed nucleation mixture: 10% glycerol, 1× BRB80, 1 mM GMPCPP, 0.8 mM DTT, 4.8 μM bovine tubulin, 0.4 μM biotinylated tubulin.
5. Incubate 1 h at 37 °C, then snap freeze in 15 μL aliquots. Store at −80 °C. When seeds are needed, quickly thaw an aliquot and place in a 37 °C water bath until use.
6. Check seeds by visualizing product using ve-DIC (look for microtubules 1–3 μm in length). Their nucleation capacity can be tested by growing microtubules from bovine brain tubulin according to, "Preparing coverslip-anchored microtubules with side-bound microbeads" (*see* Subheading 3.5 below), optionally omitting the beads.

3.3 Anti-His Bead Preparation

1. In a 500 μL eppendorf tube, mix 145 μL of MQ-H_2O, 53 μL 5× BRB80 and 22.5 μL 440 nm streptavidin-coated polystyrene beads.
2. Sonicate in ice-water bath for 5 min, to break up bead clumps that tend to form in the concentrated bead stock. We use a custom jig made of wire to hold a 500 μL eppendorf tube directly in front of the ½-in. sonicator tip. Both tube and tip are submerged in ice-water during sonication to minimize heating.
3. Mix sonicated beads with 4.5 μL Penta-His biotin conjugate, set on rotator at 4 °C for 1 h to allow binding of biotinylated antibodies to streptavidin on the beads.
4. Make assay buffer (AB) (1.5 mL 40 mg/mL BSA, 1.5 mL 5× BRB80, 4.5 mL MQ-H_2O, 7.5 μL 1 M DTT). Filter at 0.1 μm. Final assay buffer concentration: 8 mg/mL BSA, 1× BRB80, 1 mM DTT.
5. Increase the volume of bead mix to 500 μL by adding 275 μL of AB.
6. Resuspend gently, sonicate 1 min and resuspend again to encourage bead clumps to break apart and ensure the bead mix is as homogenous as possible.
7. Spin at 16,000 RCF for 9 min at 4 °C to separate beads from antibody-containing solution. Gently aspirate and discard supernatant, leaving just enough to keep bulk of pellet hydrated. Quickly resuspend pellet in 500 μL AB. Sonicate 1 min.
8. Repeat **step 7** five times. At the last resuspension, resuspend pellet to make a final volume of 225 μL. Final concentrations in the anti-His bead mixture: 8 mg/mL BSA, 1× BRB80, 1 mM DTT, ~60 pM 440-nm polystyrene beads.
9. Store Anti-His beads on tube rotator at 4 °C, rotating continuously for up to 1 month. Ensure that the beads are freely dispersed in solution prior to use (*see* **Note 2**).

3.4 Preparing Disposable Channel Slides

1. Place a microscope slide on a clean, flat surface.
2. Lightly stretch 3-in. strips of ¼-in. wide double-stick tape, adhering the tape perpendicular to the long axis of the microscope slide to define channel boundaries. Three strips of tape should allow construction of two 1-mm wide channels (Fig. 3).
3. Trim the tape at the edge of the microscope slide with a razor blade.
4. Lightly adhere a KOH-cleaned coverslip to the tape pattern on the microscope slide, orienting the long dimension of the coverslip orthogonally to the long dimension of the slide.

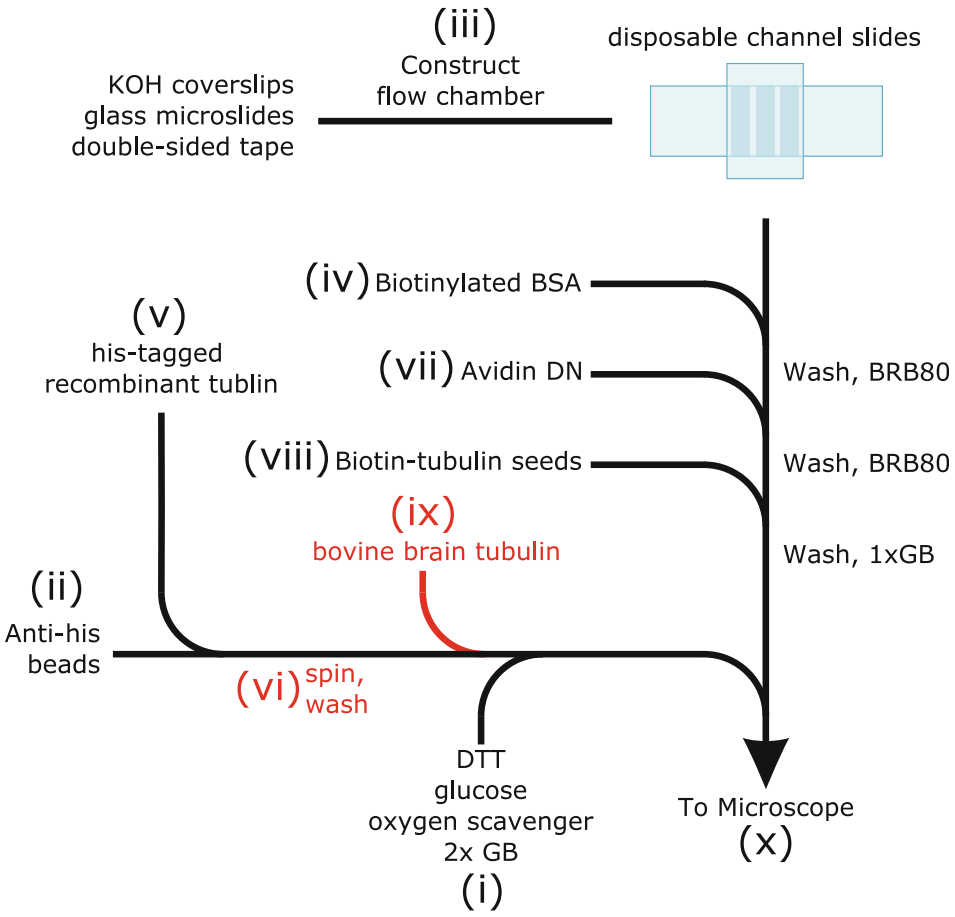

Fig. 3 Order of operations for preparing coverslip-anchored microtubules with side-bound microbeads. (i) Buffers and reaction mixes are prepared. (ii) Anti-His beads are passivated and washed. (iii) A disposable channel slide is constructed. (iv) Warm biotinylated BSA is added to the disposable channel slide. (v) His-tagged recombinant tubulin is clarified. (vi) (optional step for bovine brain tubulin wave assay) His-tagged, clarified yeast tubulin is incubated with anti-His beads. Subsequently these beads are washed and resuspended. (vii) BSA is washed from the disposable channel slide, and warm avidin is introduced and incubated on the slide. (viii) Avidin is washed from the disposable channel slide, and warm biotin-tubulin microtubule seeds are incubated on the slide. (ix) (optional for bovine brain tubulin wave assay) bovine tubulin is added to the reaction mix. (x) The slide is washed with 1× growth buffer (1× GB), and reaction mix containing anti-His beads decorated with recombinant tubulin, free tubulin, reducing agent, oxygen scavenger system, and GTP is added to the disposable channel slide. Subsequently the slide is sealed to prevent evaporation and mounted on the trapping microscope

Both ends of the coverslip should extend past the edges of the microscope slide. These coverslip extensions, when the slide is held in a coverslip-down orientation, serve as platforms onto which solutions can be pipetted for loading into the channels.

5. Use a 1 mL pipette tip to press down, and back and forth on areas of the glass-tape sandwich to fully seal the chamber sides.
6. Place the newly constructed chamber in a heated oven at 55 °C for at least 10 min prior to filling chambers with buffers (*see* **Note 3**).

3.5 Preparing Coverslip-Anchored Microtubules with Side-Bound Microbeads

The steps below describe how to produce a slide sparsely decorated with coverslip-anchored dynamic microtubules, with beads tethered to the sides of some microtubules. The wave assay developed in our lab originally relied entirely on recombinant, His-tagged yeast tubulin. We have since adapted our approach to allow other tubulin sources to be used, including untagged, native brain tubulin. Incorporating untagged tubulin requires some additional steps, which are indicated as optional below.

1. Place TLA-100 rotor with two tubes on cold-block in 4 °C fridge. Turn on ultracentrifuge, set to 4 °C, turn on vacuum.
2. Prepare two 1 mL aliquots of 1× BRB80. Place one on ice, one at 37 °C.
3. Prepare 120 μL 40 mg/mL BSA from high-concentration stock. Place on ice.
4. Prepare 50 μL 40 mM DTT. Store either at room temperature or on ice.
5. Prepare 2× growth buffer (2× GB): Mix 21 μL MQ-H_2O, 48 μL 5× BRB80, 48 μL 40 mg/mL BSA, 3 μL 100 mM GTP. Place on ice.
6. Prepare 1× GB: Mix 50 μL 2× GB, 50 μL MQ-H_2O. Place on ice.
7. Prepare reaction mix (RXN) (Fig. 3i): Mix 25 μL 2× GB, 1 μL 40 mM DTT, 1 μL 2.4 M glucose.
8. Make bead dilution (Fig. 3ii): Mix 5 μL 40 mg/mL BSA, 5 μL biotinylated BSA, 17.5 μL anti-His beads (*see* **Note 4**). Sonicate for 5 min on ice at 8 intensity, constant pulse. Incubate for 25 min, rotating at 4 °C.
9. Make flow chamber with KOH-cleaned coverslip and double-stick tape according to instructions in Subheading 3.4 (Fig. 3iii). Warm in 55 °C oven for 15 min.
10. Add 35 μL of biotinylated BSA (BBSA) to an empty eppendorf tube, incubate at 37 °C. Add 35 μL of Avidin DN to another empty eppendorf tube, incubate at 37 °C.
11. Initialize microscope: Turn on Hg-arc lamp, trap laser, set trap laser power, turn on cutting laser.
12. Coat channel surfaces with biotinylated BSA (Fig. 3iv): Add 15 μL BBSA to each lane on a slide fresh from oven, aspirating from one end of a channel to pull 15 μL through. Place the filled slide in a humid slide box, avoiding dirtying the coverslip via contact with other surfaces, and incubate for 15 min.
13. Clarify tubulin (Fig. 3v): When bead dilution mix from **step 8** above has incubated for ~17 of its full 25 min, spin recombinant yeast tubulin in cold TLA-100 rotor at 330,000 RCF, 4 °C, 10 min in ultracentrifuge.

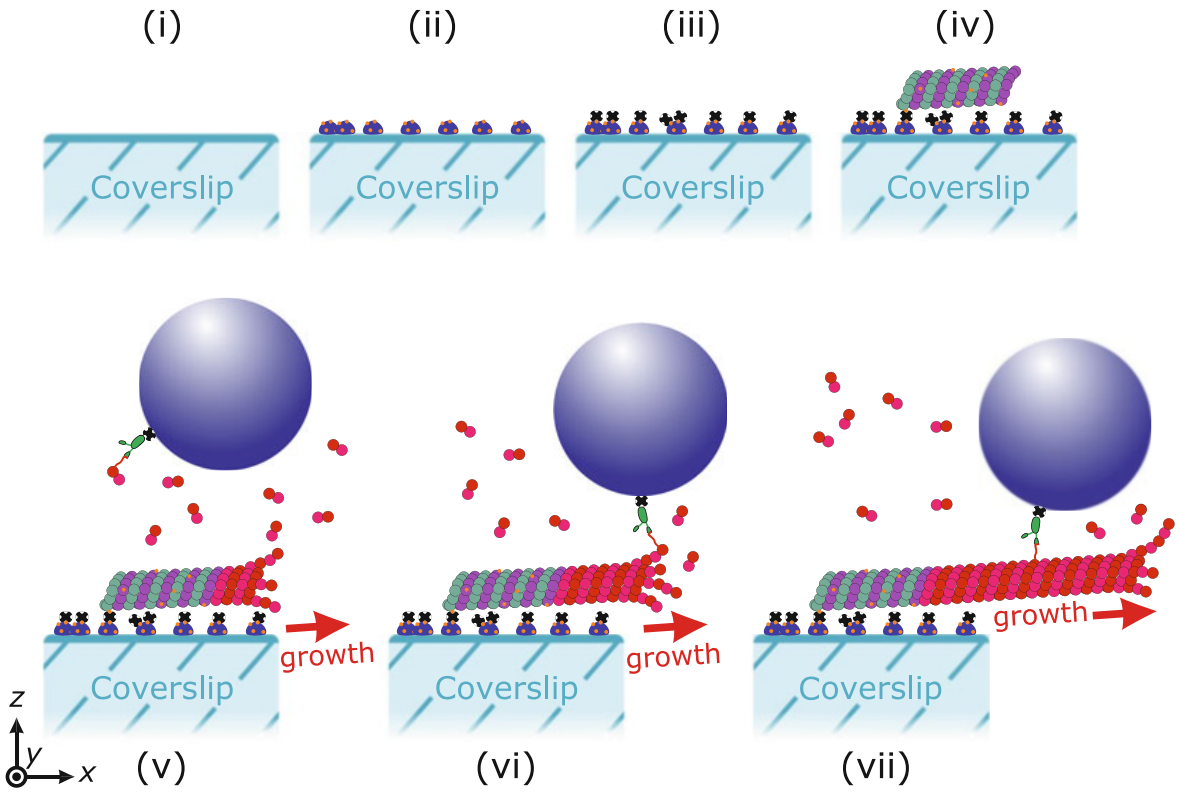

Fig. 4 Tubulin-decorated beads become incorporated into growing microtubule tips. (i) A clean disposable channel slide is constructed. (ii) Biotinylated bovine serum albumin (BBSA) is flowed into the chamber, and nonspecifically adsorbs to the clean surface (purple dots). (iii) Avidin DN (black squares) is flowed into the chamber and binds to BBSA already adhered to the slide surface. (iv) Biotinylated GMPCPP-stabilized short microtubules "seeds" made from bovine brain tubulin (purple and green) are flowed into the chamber and bind to the avidin DN on the surface. These seeds serve as nucleation points for further microtubule growth. (v) Streptavidin-coated beads (blue) are sparsely decorated with biotinylated anti-His antibody (green), through which they bind free His-tagged recombinant yeast tubulin. A reaction mixture containing the decorated beads together with free recombinant yeast tubulin (pink and red) is flowed into the chamber. Microtubule extensions composed of the recombinant tubulin grow from the coverslip-anchored seeds. (vi) The bead-bound tubulin incorporates into growing microtubules at their assembling tips. (vii) Microtubule assembly continues past the beads, converting tip-attached beads into side-attached beads. All elements are drawn approximately to scale except the beads, which are at one-fourth relative scale to accommodate inclusion in the diagram

14. Make tubulin-decorated beads (Fig. 3vi, skip this step if performing an assay with recombinant, His-tagged tubulin alone): When bead dilution from **step 8** has incubated for its full 25 min, add 5–10 μL of 2–7 μM yeast tubulin directly from rotor to bead dilution, pipetting from the center of the supernatant to avoid accidentally collecting any pelleted debris. Mix gently but thoroughly by pipetting and incubate 10 min at 4 °C, rotating, to allow binding of His-tagged recombinant tubulin to anti-His antibodies on beads. Final concentrations

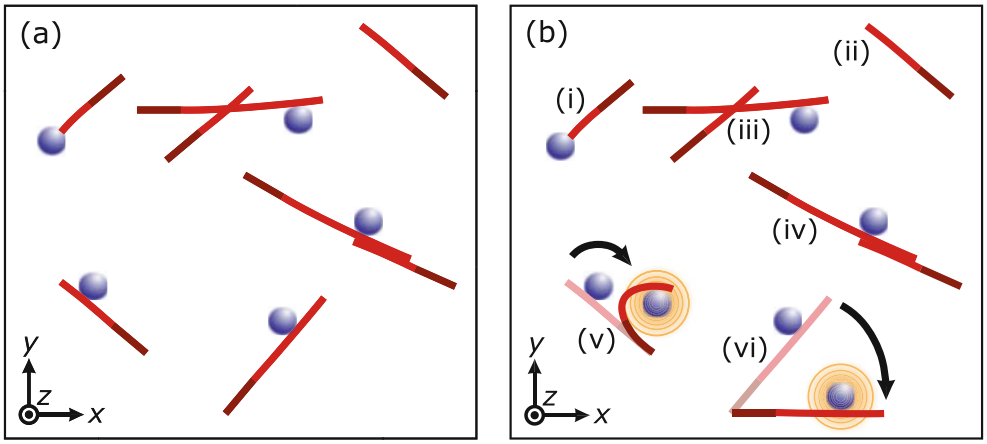

Fig. 5 Selecting a microtubule-bead pair suitable for measurement. (**a**) Top-down view of a typical slide as prepared by the protocol in Subheading 3.5. Coverslip-anchored biotinylated microtubule seeds (dark red) nucleate dynamic microtubule extensions polymerized from recombinant His-tagged yeast tubulin (red). Tubulin-decorated beads (blue) become incorporated into growing microtubules. (**b**) The measurements detailed in Subheading 3.6 require a coverslip-anchored microtubule to have a side-attached bead, and be free from the mechanical influence of other microtubules. (i) This microtubule-bead pair has a bead end-bound to the microtubule, and therefore it is not a suitable choice for measurement. (ii) This microtubule has no attached bead. (iii) Although this microtubule does have a side-attached bead, another microtubule crosses along its length, potentially interfering with the measurements. The interfering microtubule might be carefully trimmed away using laser scissors. (iv) This microtubule-bead pair is bundled with another microtubule, preventing re-orientation. The interfering microtubule might be carefully trimmed away using laser scissors. (v) This microtubule-bead pair is properly isolated and has a suitable side-attached bead, but it is not oriented along the measurement axis (*x*-axis) and the seed is anchored too firmly to the coverslip, such that it cannot be reoriented by manipulation with the laser trap (orange). (vi) This isolated microtubule-bead pair is anchored to the coverslip and able to be reoriented for measurement along the *x*-axis (motion to measurement axis is represented by black arrow). *See* Subheading 3.6 for details

in bead-decoration mix: 0.5–1 μM yeast tubulin, ~30 pM beads, ~0.6× BRB80, ~10 mg/mL BSA.

15. Wash tubulin-decorated beads (Fig. 3vi, skip this step if performing an assay with recombinant, His-tagged tubulin alone): Simultaneous with slide incubation, spin tubulin-decorated beads at 4 °C, in cold benchtop centrifuge at 16,000 RCF, 10 min. Discard supernatant (try to keep beads from contacting air), resuspend in 27.5 μL cold 1× GB + 1 μL BBSA.
16. Coat channel surfaces with avidin (Fig. 3vii): After slide prepared in **step 12** above has incubated (with BBSA) for its full 15 min, wash each lane with 80 μL warm 1× BRB80. Add 15 μL of avidin DN to each lane. Incubate slide in humidity chamber for 5 min.
17. Retrieve biotin-tubulin microtubule seeds from −80 °C freezer, transfer quickly to 37 °C.

18. Decorate channel surfaces with microtubule seeds (Fig. 3viii): Wash each lane with 40 μL warm 1× BRB80. Dilute 1–10 μL of warm microtubule seeds in 50 μL BRB80 (according to desired density of microtubule seeds on slide surface). Add 15 μL diluted seeds to each lane and incubate for 5 min in humidity chamber. Warm 1× GB by placing on 37 °C block.
19. Remove any unbound microtubule seeds by washing each lane with 20 μL warm 1× GB. Incubate slide in humidity chamber.
20. Finish reaction mix (Fig. 3ix): To RXN from **step 7** above, add tubulin (to a target concentration of 12–20 μM for bovine tubulin, or 1.5–3 μM for yeast tubulin), 4 μL of bead dilution, 1 μL of 100× oxygen scavenger, and enough cold 1× BRB80 to bring the final volume to 50 μL. Mix thoroughly by pipetting. Final concentrations in reaction mix: 1× BRB80, 8 mg/mL BSA, 1 mM DTT, 12–20 μM bovine tubulin or 1.5–3 μM yeast tubulin, ~3 pM beads, 1 mM GTP, 1 mM DTT, 25–50 mM glucose, ~200 μg/mL glucose oxidase, ~35 μg/mL catalase.
21. Add reaction mix to chamber, seal edges with nail polish (Fig. 3x). Mount the slide on the optical trap. Monitor the coverslip surface by ve-DIC for microtubule growth from coverslip-anchored seeds and free-floating tubulin-decorated beads. Tubulin-decorated beads become incorporated into microtubules at their growing tips, remaining attached at their point of incorporation as the microtubule continues to grow (Fig. 4). Such beads are observed subsequently as side-attached to a coverslip-anchored, growing microtubule.

Several aspects of the preparation must be optimized to produce a sufficient number of coverslip-anchored microtubules with side-attached beads that do not contact other microtubules. First, the density of microtubule seeds on the surface should be tuned low enough to mitigate microtubules contacting each other during growth, but high enough so the tubulin-decorated beads can encounter and incorporate into growing tips. Moreover, the concentration of free tubulin should be tuned high enough that microtubules are predominantly in their growth regime, with catastrophes minimized, but not so high that overgrowth leads to significant contact of microtubules with each other (crossing or bundling). Lastly, we use the concentration of anti-His antibody to tune the amount of tubulin on the surface of the tubulin-decorated beads. If beads are decorated too densely with tubulin, then their binding to a growing tip can inhibit further polymerization, and most microtubule-bound beads are seen in a "lollipop" configuration, without any microtubule extension past the bead (*see* Fig. 5). Additionally, heavily decorated beads can also inhibit depolymerization past the point of bead tethering. We suspect that

multiple attachments between the bead and the microtubule stabilize the lattice. In either case, these configurations are unusable in the wave assay. The amount of tubulin on beads may be tuned down to the single-molecule level by adjusting the antibody level (in Subheading 3.3, **step 3**, above) such that only 50% of beads bind when held in contact with a growing microtubule tip (this procedure is documented in ref. 29).

Tubulin aliquots should be thawed quickly (e.g., by holding in-hand), kept on ice until used, and used as soon after thawing as possible. In our experience, tubulin of all types can be prone to aggregation, and aggregation increases with time, temperature, and concentration. We include a clarifying ultracentrifugation step in this protocol to eliminate aggregate sometimes present in freshly thawed yeast tubulin samples. When large aggregates are present on a slide, we observe heavy decoration of the aggregates with anti-His beads and time-dependent depletion of free beads from solution. We therefore suspect tubulin aggregates act as sinks for anti-His beads, effectively limiting the time over which measurements can be made. In addition, aggregates can fall into the trap, directly interfering with the measurements. Therefore, depending on the particular lab setup and experimental practices, we recommend adjusting the timing of **steps 13–15** and **20** above (in Subheading 3.5) to minimize the time between thawing and using tubulin, and to minimize instances where tubulin aliquots are above 4 °C.

3.6 Measuring Pulses of Motion Generated by Curling Protofilaments

The optical trap setup used for this assay is described in previous work [31]. Briefly, a 1064-nm laser is used as a trapping beam, and a 473-nm laser as a microtubule cutting beam. The 1064-nm laser is focused at the center of the field of view. The 473-nm cutting laser is focused into an ellipse at an intermediate distance between the trap center and the edge of the field of view. Both lasers are actuated independently by shutters. To measure pulses generated by protofilaments curling outward from disassembling microtubule tips:

1. Identify a suitable bead laterally attached to a microtubule (Fig. 5). This microtubule should be firmly anchored to the slide surface, without other interfering microtubules bundled alongside or crossing along its length. The microtubule will need to be oriented such that its plus end intersects with the cutting beam. Suitable microtubules with side-bound beads are sometimes found already in this orientation. However, in cases where an otherwise suitable microtubule is misoriented, we often find that by using the trap it is possible to reorient them by swiveling them about their coverslip-anchor. The cutting laser can also sometimes be used to trim away interfering microtubules.

2. Establish initial loaded state: Trap the laterally attached bead and pull the microtubule and bead toward cutting laser. Raise the bead slightly above the coverslip surface to ensure the surface does not interfere with the measurement. Turn on the force clamp, placing the bead and microtubule under tension, with the plus end of the microtubule passing though the cutting region.
3. Initiate microtubule depolymerization by trimming off the stabilizing cap of the microtubule using the cutting laser. Record position signals from the trapped bead using the force clamp software. When the bead detaches from the microtubule, stop the force clamp software and make relevant notes for the bead-microtubule pair.

3.7 Analyzing Wave Assay Data

Our optical traps use a simple stage-based feedback-control. Therefore, the stage and bead position signals encode the pulse data to be analyzed. Bead-trap separation encodes the level of force, is sampled at 40 kHz, and then decimated to 200 Hz for recording. The stage position encodes bead movement relative to the coverslip and is updated and recorded at 50 Hz. Each pulse event is captured with a 10–20 s recording of the stage and trap separation signals.

Our custom analysis software (written in IGOR Pro, Wavemetrics) facilitates data analysis and is available upon request. However, wave assay data can be analyzed relatively easily using any data processing software. Briefly, the stage position along the x-axis (parallel with the microtubule axis) is plotted against time to visualize microtubule disassembly-driven pulses (Fig. 6). A pulse can be parameterized by its amplitude, risetime, and ability to be differentiated from baseline noise. We define pulse amplitude as the difference between the maximum value at the peak and the arithmetic mean of at least 2 s of the signal directly prior to the pulse. We require an amplitude of at least three times the RMSD of the baseline noise for a candidate pulse to be considered valid (Fig. 7). Pulse amplitudes for recombinant yeast tubulin range from 40 to 100 nm, well above the mean baseline noise (RMSD $\approx$ 4 nm), making them easily distinguishable. Pulse risetimes (i.e., the times for the pulses to depart from the baseline and reach their maximum value) typically range from 100 to 400 ms [29].

By enabling measurements of pulse properties as functions of force, the wave assay provides a unique window into both the mechanics and thermodynamics of microtubule tip disassembly. Pulse amplitudes, measured in the wave assay using yeast tubulin alone, decrease as the force of the laser trap is increased (Fig. 8), demonstrating directly that curling protofilaments behave like springs. The area under the pulse amplitude vs. force curve (which is independent of geometric details such as bead size [29])

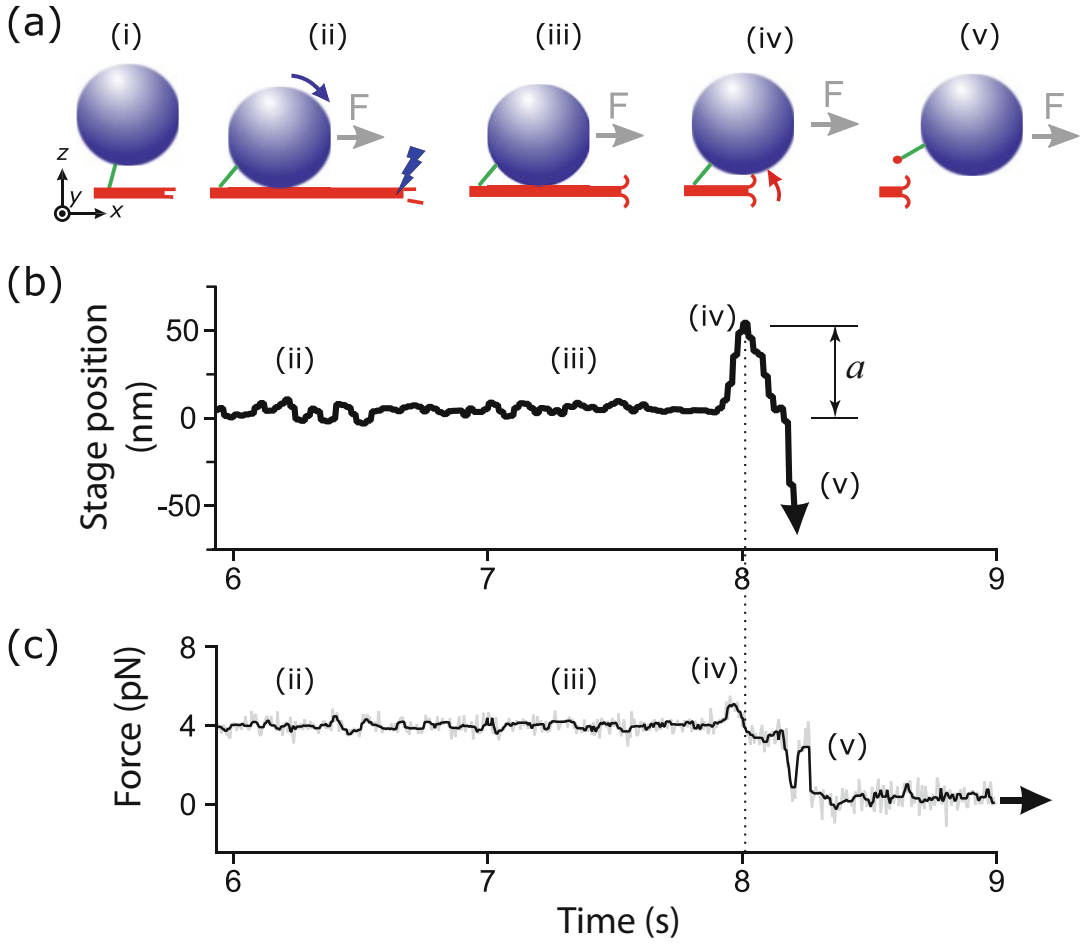

Fig. 6 Measuring pulses of bead motion generated by curling protofilaments. (**a**) Sequence of events during a typical wave measurement: (i) Side-attached bead on a coverslip-anchored microtubule. (ii) The bead-microtubule is maneuvered to be oriented along the *x*-axis (the measurement axis) and is pulled opposite the direction of the coverslip-anchored seed with a force of 4 pN. This pulling force presses the bead against the body of the microtubule. Data acquisition is initiated, and then the end of the microtubule is trimmed off with laser scissors to initiate microtubule depolymerization. (iii) The microtubule depolymerizes toward the tensioned bead. (iv) When the depolymerizing microtubule tip reaches the location where the bead makes contact with the microtubule, protofilament curls push on the bead, causing it to rock back about its tether. (v) The microtubule continues to depolymerize past the bead-tether, releasing the bead from the microtubule. The force clamp program attempts to maintain the requested load force, and therefore pulls the detached bead rapidly away from the measurement location. (**b**) The stage position is plotted vs. time. The amplitude of the pulse is denoted by *a*. (**c**) The trap force is plotted vs. time. The force clamp is able to maintain the requested 4 pN load force, even during the 130-ms protofilament curl-induced pulse of motion. The trap force falls to zero rapidly once the bead is completely detached from the microtubule

represents the total available mechanical work output, W, from the subset of curling protofilaments that push against the microbead. The total available work output measured using yeast tubulin, $W \approx 300$ pN nm, is a very substantial amount of mechanical energy, roughly 70-fold greater than thermal energy ($k_B T = 4.1$ pN nm) [29]. This large capacity for work output in the wave assay can be

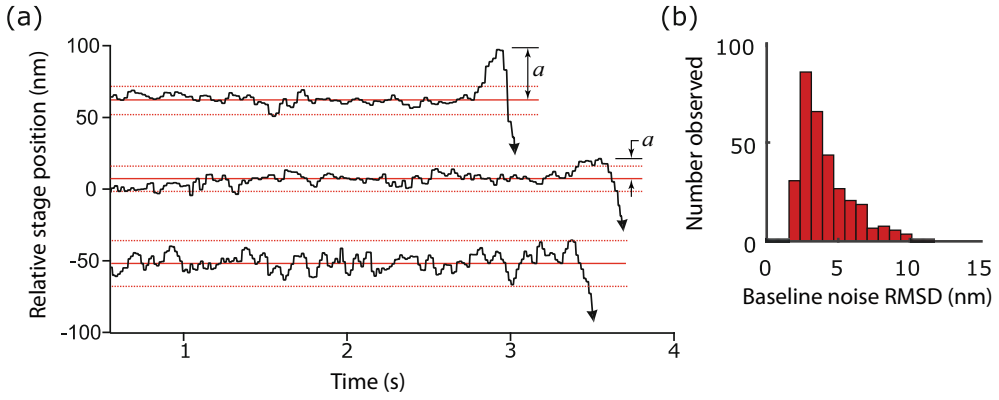

Fig. 7 Distinguishing wave assay pulses from noise. (**a**) Plot of three relative stage position traces over time. The baseline noise is characterized by the mean position (solid red line) computed over a 2-s window preceding a candidate pulse. The noise magnitude is bounded well by an interval (dotted red lines) defined by ± 3 times the root-mean-square-deviation ($\pm 3\times$ RMSD) of the position signal around its baseline. Each pulse can then be parametrized by a risetime, usually between 100 and 500 ms and an amplitude, typically 6–100 nm, denoted here by *a*. (i) The first trace shows a pulse clearly distinguishable from the baseline noise, with a peak well above the $3\times$ RMSD threshold. (ii) The second trace shows a pulse just satisfying the $3\times$ RMSD criterion. (iii) The third pulse does not satisfy the $3\times$ RMSD criterion, and is therefore rejected from aggregation into statistics of wave assay pulses. (**b**) The distribution of the baseline noise RMSD (from $N = 318$ recorded events) shows a mode around 3 nm, with a long tail due to rarer high-noise traces. The distribution shows that pulses of ~10 nm are usually detectable above the $3\times$ RMSD criterion. Because the minimum RMSD is ~2 nm, the absolute minimum detectable pulse amplitude is ~6 nm. Small pulses, with amplitudes below 10 nm, are likely to be missed, potentially skewing the mean pulse amplitude toward a higher value. In cases where a large fraction of events fail to produce detectable pulses, or where the pulse amplitudes are very close to the detection threshold, the median or mode might be better summary statistics

related to fundamental thermodynamic properties, such as the energy per tubulin dimer, given estimates for the fraction of protofilaments and the number of tubulin dimers that push against the bead in the assay. Based on the geometry of the bead and tether, we estimate that a maximum of four protofilaments could push simultaneously against the bead (Fig. 9), which implies that W represents only about one-third of the total mechanical energy available from the entire disassembling tip (4 out of 13 protofilaments, or 31%). Based on the morphological characteristics of curling protofilaments seen in electron micrographs [35, 38, 39], we infer that curling protofilaments typically contain about four tubulin dimers, which suggests a maximum of 16 tubulin dimers (4 curls with 4 dimers each) might contribute to W and therefore that the strain energy per tubulin dimer is at least 19 pN nm (i.e., W divided by 16). We consider this estimate a lower bound, because it assumes simultaneous pushing by four protofilaments, which might not always occur. Nevertheless, it corresponds to approximately 22% of the total energy available from GTP hydrolysis. We also note that the geometric arrangement of the bead, tether, and microtubule in the wave assay creates a lever system that amplifies protofilament

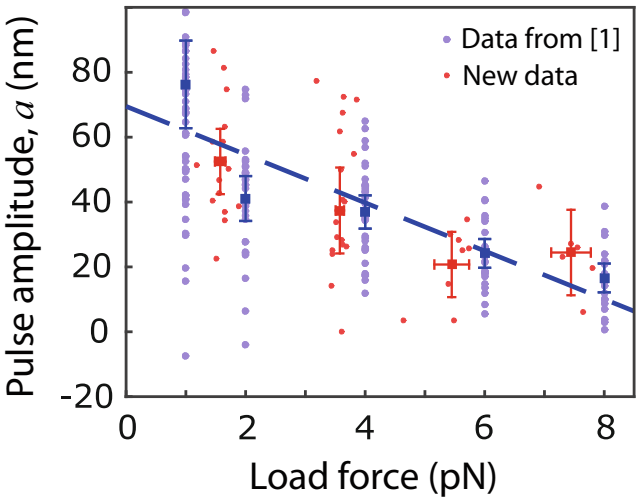

Fig. 8 Protofilament curls are spring-like and release a substantial amount of mechanical energy during microtubule disassembly. Pulse amplitude plotted vs. trapping force. Data are plotted as individual pulses (small dots) and means for each load force (squares). Force suppresses pulse amplitudes, indicating that protofilaments are spring-like. The area under the fit line ($W \approx 300$ pN nm) represents the total mechanical work output available from the subset of curling protofilaments that push against the microbead in the assay. Data reported previously [29] are plotted in blue. New data, recorded independently and reproducing the same trend, are plotted in red. Error bars represent 95% confidence intervals, defined as $\pm$ (t·SEM), where t is drawn from the Student's t-distribution (with $\nu = N - 1$ degrees of freedom and $N = 6$–58 samples per mean)

curl motions by a modest amount that is sensitive to tether length and bead size (Fig. 9a, b, [29]).

The energetic estimates obtained here using the wave assay show that protofilament curls are powerful and carry a substantial amount of energy in the form of curvature strain. Rigorously testing whether this mechanical energy is harnessed by kinetochores and other microtubule tip-couplers is an area for future work. The wave assay will be useful for this endeavor, because of its unique ability to directly assess the mechanical strain energy released by curling protofilaments, and to test strategies for altering this strain energy. More generally, the assay should enable new studies of the mechanochemistry of native tubulins purified from different organisms (Fig. 10) and recombinant tubulins carrying various mutations.

4 Notes

1. If an ultracentrifuge is not accessible, an alternative option for clarifying tubulin is to use 0.1 μm centrifugal spin filters (e.g.,

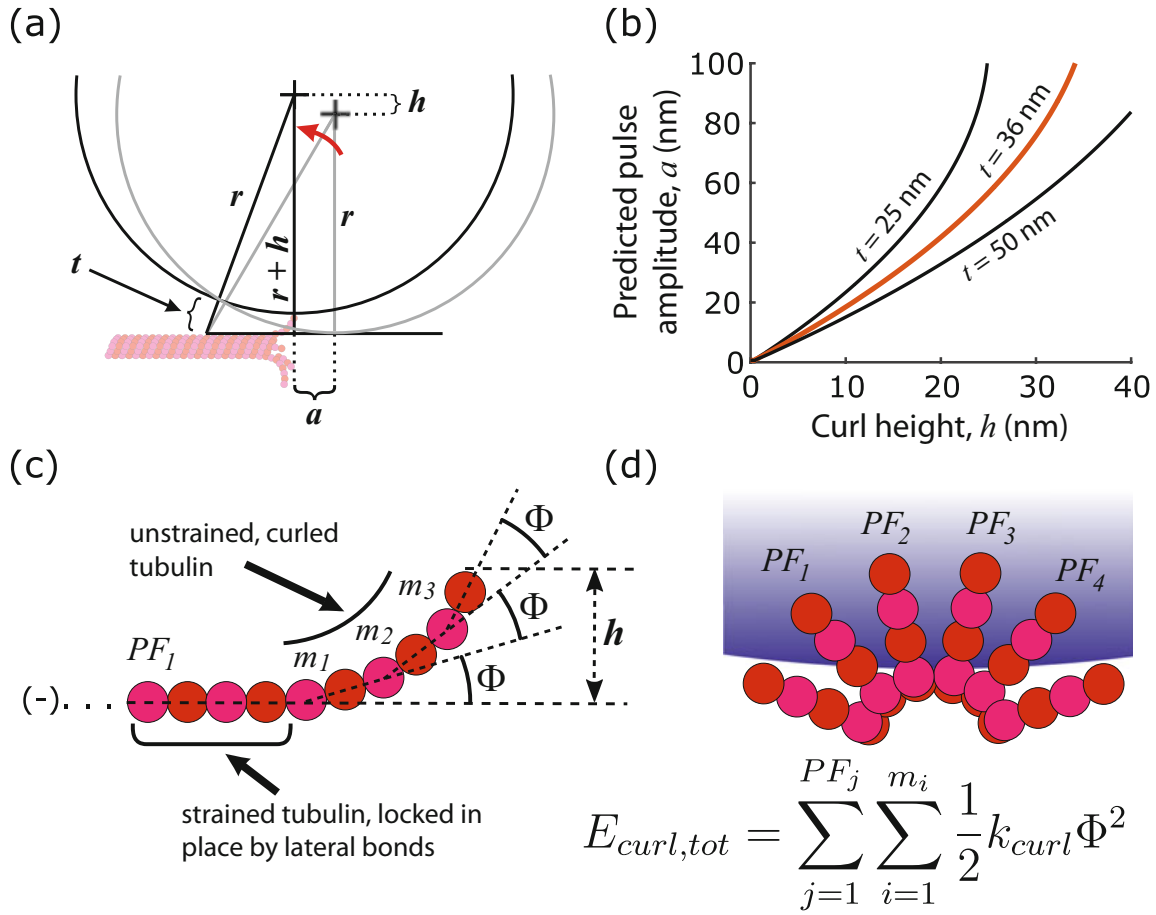

Fig. 9 Leverage in the wave assay and how curl properties can be related to measured wave energies. (**a**) The arrangement of the bead and its engineered tether creates a mechanical lever system that modestly amplifies the motion of the curling protofilaments. The relationship between the measured pulse amplitude, *a*, and the protofilament curl height, *h*, depends on the tether length, *t*, and the bead radius, *r*. (**b**) The predicted *a*-vs.-*h* relationship for tether lengths of $t = 25$, 36, and 50 nm, assuming a bead radius of $r = 220$ nm. At the tether length we estimate for our assay, $t = 36$ nm, protofilament curl motions are amplified between 2- and 2.5-fold. For all tether lengths, the *a*-vs.-*h* relationship is approximately linear until the curl height approaches the tether length, at which point significant nonlinearities arise. (**c**) Parameterization of protofilament curl morphology. Protofilament height, *h*, is a function of the number of tubulin dimers in the protofilament (contour length) and the mean angle per dimer, Φ. These morphological parameters can be estimated from cryo-electron micrographs and tomograms of disassembling microtubule tips [35–37]. (**d**) End-view of a disassembling microtubule tip, indicating that up to four protofilaments could push on a tethered bead. The equation below relates curl energy to protofilament morphological parameters and the mean stiffness per dimer, k_{curl}

EMD-Millipore cat# UFC30VV). However, these filters have been associated with ~50% tubulin loss in our hands.

2. Over time, older stocks of Anti-His beads can sometimes form a web-like precipitate, which has been associated with beads that do not perform as expected in assays.
3. This heating step helps adhere tape to glass surfaces. If adhesion is poor, then solutions are gradually pulled by capillary

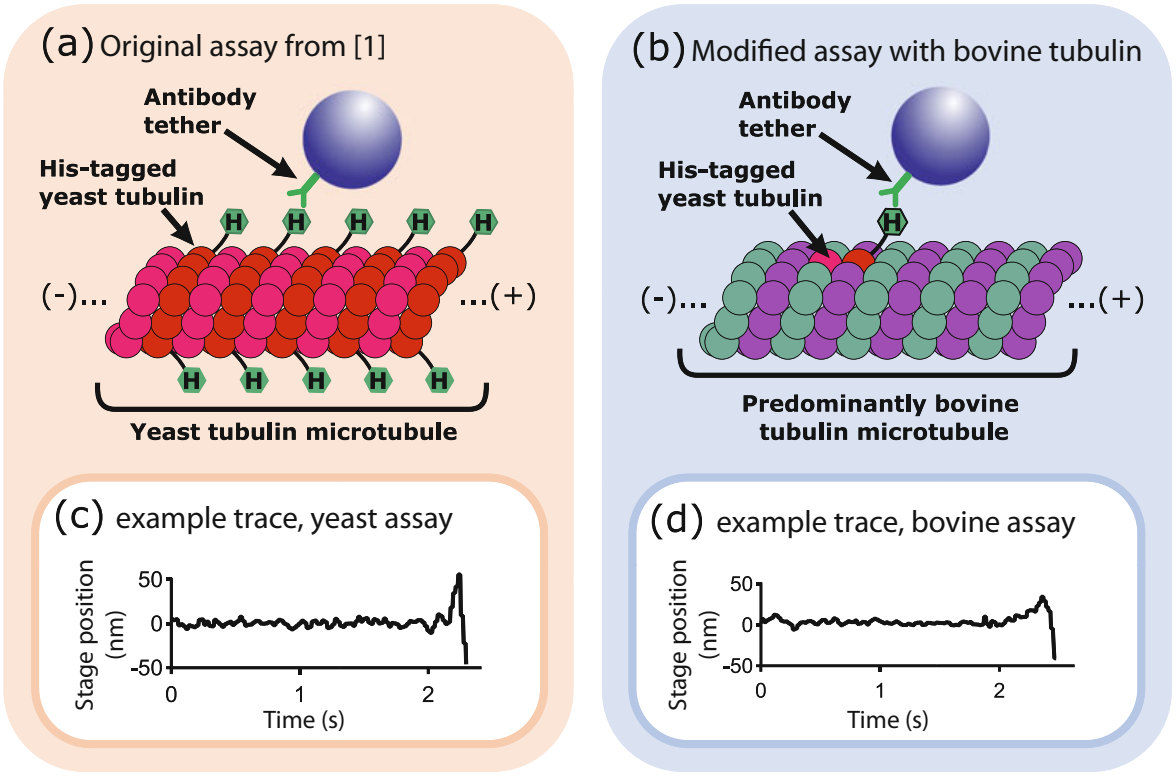

Fig. 10 Comparison of wave assay and modifications to allow pulses to be measured from untagged tubulin. (**a**) Schematic of our original wave assay [29]. Beads functionalized with anti-penta-His antibody bind free, recombinant His-tagged yeast tubulin, through which they are tethered to microtubules composed of the same, recombinant yeast tubulin. (**b**) Schematic of our modified assay for measuring conformational waves generated by untagged tubulin. Beads functionalized with anti-penta-His antibody are first decorated sparsely with His-tagged yeast tubulin and then mixed with untagged tubulin (e.g., purified from bovine brain). The beads become tethered when bead-bound His-tagged tubulin incorporates into growing microtubules composed predominantly of untagged tubulin. (**c**) Example pulse generated by a microtubule composed entirely of recombinant, His-tagged yeast tubulin. (**d**) Example pulse generated by a microtubule composed predominantly of native bovine brain tubulin

action out of the channel and into small gaps between the tape and glass. In extreme cases, this effect can eventually completely dry a channel and ruin an experiment.

4. Including biotinylated BSA is important during this incubation step to ensure that any remaining streptavidin, not already bound to biotinylated anti-His antibody, becomes occupied. Fully occupying all the streptavidin prevents direct binding of the beads to biotinylated coverslip-anchored microtubule seeds, an arrangement that would be difficult to distinguish from the desired tethering, where beads are attached via anti-His antibodies and C-terminal tubulin tails to the sides of microtubule extensions.

Acknowledgments

Work in the C.L.A. lab is currently supported by the NIH (R35GM134842) and by the Packard Foundation (Fellowship 2006-30521). Work in the L.M.R. lab is supported by the NIH (R01GM098543), the NSF (MCB-2017687), and the Robert A Welch Foundation (I-1908).

References

1. Ashkin A, Dziedzic JM, Bjorkholm JE, Chu S (1986) Observation of a single-beam gradient force optical trap for dielectric particles. Opt Lett 11(5):288–290. https://doi.org/10.1364/ol.11.000288
2. Nicholas MP, Rao L, Gennerich A (2014) An improved optical tweezers assay for measuring the force generation of single kinesin molecules. Methods Mol Biol 1136:171–246. https://doi.org/10.1007/978-1-4939-0329-0_10
3. Lang MJ, Asbury CL, Shaevitz JW, Block SM (2002) An automated two-dimensional optical force clamp for single molecule studies. Biophys J 83(1):491–501. https://doi.org/10.1016/s0006-3495(02)75185-0
4. Gennerich A, Carter AP, Reck-Peterson SL, Vale RD (2007) Force-induced bidirectional stepping of cytoplasmic dynein. Cell 131(5):952–965. https://doi.org/10.1016/j.cell.2007.10.016
5. Sommese RF, Sung J, Nag S, Sutton S, Deacon JC, Choe E, Leinwand LA, Ruppel K, Spudich JA (2013) Molecular consequences of the R453C hypertrophic cardiomyopathy mutation on human beta-cardiac myosin motor function. Proc Natl Acad Sci U S A 110(31):12607–12612. https://doi.org/10.1073/pnas.1309493110
6. Guo B, W.H. Guilford (2006) Mechanics of actomyosin bonds in different nucleotide states are tuned to muscle contraction. Proceedings of the National Academy of Sciences of the United States of America 103(26):9844–9849. https://doi.org/10.1073/pnas.0601255103
7. Vanzi F, Capitanio M, Sacconi L, Stringari C, Cicchi R, Canepari M, Maffei M, Piroddi N, Poggesi C, Nucciotti V, Linari M, Piazzesi G, Tesi C, Antolini R, Lombardi V, Bottinelli R, Pavone FS (2006) New techniques in linear and non-linear laser optics in muscle research. J Muscle Res Cell Motil 27(5–7):469–479. https://doi.org/10.1007/s10974-006-9084-3
8. Wang MD, Schnitzer MJ, Yin H, Landick R, Gelles J, Block SM (1998) Force and velocity measured for single molecules of RNA polymerase. Science 282(5390):902–907. https://doi.org/10.1126/science.282.5390.902
9. Abbondanzieri EA, Greenleaf WJ, Shaevitz JW, Landick R, Block SM (2005) Direct observation of base-pair stepping by RNA polymerase. Nature 438(7067):460–465. https://doi.org/10.1038/nature04268
10. Smith DE, Tans SJ, Smith SB, Grimes S, Anderson DL, Bustamante C (2001) The bacteriophage phi 29 portal motor can package DNA against a large internal force. Nature 413(6857):748–752. https://doi.org/10.1038/35099581
11. Aubin-Tam M-E, Olivares AO, Sauer RT, Baker TA, Lang MJ (2011) Single-molecule protein unfolding and translocation by an ATP-fueled proteolytic machine. Cell 145(2):257–267. https://doi.org/10.1016/j.cell.2011.03.036
12. Gore J, Bryant Z, Stone MD, Nollmann MN, Cozzarelli NR, Bustamante C (2006) Mechanochemical analysis of DNA gyrase using rotor bead tracking. Nature 439(7072):100–104. https://doi.org/10.1038/nature04319
13. Koshland DE, Mitchison TJ, Kirschner MW (1988) Polewards chromosome movement driven by microtubule depolymerization in vitro. Nature 331(6156):499–504. https://doi.org/10.1038/331499a0
14. Lombillo VA, Stewart RJ, McIntosh JR (1995) Minus-end-directed motion of kinesin-coated microspheres driven by microtubule depolymerization. Nature 373(6510):161–164. https://doi.org/10.1038/373161a0
15. Inoue S, Salmon ED (1995) Force generation by microtubule assembly disassembly in mitosis and related movements. Mol Biol Cell 6(12):1619–1640
16. Dogterom M, Yurke B (1997) Measurement of the force-velocity relation for growing microtubules. Science 278(5339):856–860. https://doi.org/10.1126/science.278.5339.856

17. Kerssemakers JWJ, Munteanu EL, Laan L, Noetzel TL, Janson ME, Dogterom M (2006) Assembly dynamics of microtubules at molecular resolution. Nature 442(7103): 709–712. https://doi.org/10.1038/nature04928
18. Cameron LA, Footer MJ, van Oudenaarden A, Theriot JA (1999) Motility of ActA protein-coated microspheres driven by actin polymerization. Proc Natl Acad Sci U S A 96(9): 4908–4913. https://doi.org/10.1073/pnas.96.9.4908
19. Footer MJ, Kerssemakers JWJ, Theriot JA, Dogterom M (2007) Direct measurement of force generation by actin filament polymerization using an optical trap. Proc Natl Acad Sci U S A 104(7):2181–2186. https://doi.org/10.1073/pnas.0607052104
20. Bieling P, Li TD, Weichsel J, McGorty R, Jreij P, Huang B, Fletcher DA, Mullins RD (2016) Force feedback controls motor activity and mechanical properties of self-assembling branched actin networks. Cell 164(1–2): 115–127. https://doi.org/10.1016/j.cell.2015.11.057
21. Aldaz H, Rice LM, Stearns T, Agard DA (2005) Insights into microtubule nucleation from the crystal structure of human gamma-tubulin. Nature 435(7041):523–527. https://doi.org/10.1038/nature03586
22. Brouhard GJ, Rice LM (2014) The contribution of alpha beta-tubulin curvature to microtubule dynamics. J Cell Biol 207(3):323–334. https://doi.org/10.1083/jcb.201407095
23. Desai A, Mitchison TJ (1997) Microtubule polymerization dynamics. Annu Rev. Cell Dev Biol 13:83–117. https://doi.org/10.1146/annurev.cellbio.13.1.83
24. Caplow M, Shanks J (1996) Evidence that a single monolayer tubulin-GTP cap is both necessary and sufficient to stabilize microtubules. Mol Biol Cell 7(4):663–675. https://doi.org/10.1091/mbc.7.4.663
25. Mickey B, Howard J (1995) Rigidity of microtubules is increased by stabilizing agents. J Cell Biol 130(4):909–917. https://doi.org/10.1083/jcb.130.4.909
26. McIntosh JR (2017) Mechanisms of mitotic chromosome segregation. MDPI, Basel
27. Asbury CL, Tien JF, Davis TN (2011) Kinetochores' gripping feat: conformational wave or biased diffusion? Trends Cell Biol 21(1): 38–46. https://doi.org/10.1016/j.tcb.2010.09.003
28. Hill TL (1985) Theoretical problems related to the attachment of microtubules to kinetochores. Proc Natl Acad Sci U S A 82(13): 4404–4408. https://doi.org/10.1073/pnas.82.13.4404
29. Driver JW, Geyer EA, Bailey ME, Rice LM, Asbury CL (2017) Direct measurement of conformational strain energy in protofilaments curling outward from disassembling microtubule tips. eLife 6:18. https://doi.org/10.7554/eLife.28433
30. Grishchuk EL, Molodtsov MI, Ataullakhanov FI, McIntosh JR (2005) Force production by disassembling microtubules. Nature 438(7066):384–388. https://doi.org/10.1038/nature04132
31. Franck AD, Powers AF, Gestaut DR, Davis TN, Asbury CL (2010) Direct physical study of kinetochore-microtubule interactions by reconstitution and interrogation with an optical force clamp. Methods 51(2):242–250. https://doi.org/10.1016/j.ymeth.2010.01.020
32. Johnson V, Ayaz P, Huddleston P, Rice LM (2011) Design, overexpression, and purification of polymerization-blocked yeast alpha beta-tubulin mutants. Biochemistry 50(40): 8636–8644. https://doi.org/10.1021/bi2005174
33. Geyer EA, Burns A, Lalonde BA, Ye XC, Piedra FA, Huffaker TC, Rice LM (2015) A mutation uncouples the tubulin conformational and GTPase cycles, revealing allosteric control of microtubule dynamics. eLife 4:20. https://doi.org/10.7554/eLife.10113
34. Castoldi M, Popova AV (2003) Purification of brain tubulin through two cycles of polymerization-depolymerization in a high-molarity buffer. Protein Expr Purif 32(1): 83–88. https://doi.org/10.1016/s1046-5928(03)00218-3
35. McIntosh JR, Grishchuk EL, Morphew MK, Efremov AK, Zhudenkov K, Volkov VA, Cheeseman IM, Desai A, Mastronarde DN, Ataullakhanov FI (2008) Fibrils connect microtubule tips with kinetochores: a mechanism to couple tubulin dynamics to chromosome motion. Cell 135(2):322–333. https://doi.org/10.1016/j.cell.2008.08.038
36. McIntosh JR, O'Toole E, Morgan G, Austin J, Ulyanov E, Ataullakhanov F, Gudimchuk N (2018) Microtubules grow by the addition of bent guanosine triphosphate tubulin to the tips of curved protofilaments. J Cell Biol 217(8): 2691–2708. https://doi.org/10.1083/jcb.201802138
37. O'Toole E, Morphew M, McIntosh JR (2020) Electron tomography reveals aspects of spindle structure important for mechanical stability at metaphase. Mol Biol Cell 31(3):184–195. https://doi.org/10.1091/mbc.E19-07-0405

38. Mandelkow EM, Mandelkow E, Milligan RA (1991) Microtubule dynamics and microtubule caps—a time-resolved cryoelectron microscopy study. J Cell Biol 114(5): 977–991. https://doi.org/10.1083/jcb.114.5.977

39. McIntosh JR, O'Toole E, Zhudenkov K, Morphew M, Schwartz C, Ataullakhanov FI, Grishchuk EL (2013) Conserved and divergent features of kinetochores and spindle microtubule ends from five species. J Cell Biol 200(4):459–474. https://doi.org/10.1083/jcb.201209154